Electronic Supplementary Material (ESI) for Physical Chemistry Chemical Physics.

Supporting Informations

Theoretical Insights into Photo-Induced Electron Transfer at BiOX(X=F, Cl, Br, I) (001) Surfaces and Interfaces

Tan Li[1], Xiaochao Zhang[1,*], Changming Zhang[1], Rui Li[1], Jianxin Liu[1],Rui Lv[1], Hui Zhang[2], Peide Han[3], Caimei Fan[1,*] Zhanfeng Zheng[4]

[1]*College of Chemistry and Chemical Engineering, Taiyuan University of Technology, Taiyuan 030024, PR China*

[2]*Particle Technology Research Centre, Department of Chemical and Biochemical Engineering, The University of Western Ontario, London, Ontario N6A 5B9, Canada*

[3]*College of Materials Science and Engineering, Taiyuan University of Technology, Taiyuan 030024, PR China*

[4]*State Key Laboratory of Coal Conversion, Institute of Coal Chemistry, Chinese Academy of Sciences*

[*]**Corresponding author**:

Xiaochao Zhang, **Caimei Fan,** College of Chemistry and Chemical Engineering, Taiyuan University of Technology, Taiyuan 030024, PR China. **Tel.**: +86-15503477962; **Fax**: +86-351-6018554. **E-mail**: zhangxiaochao@tyut.edu.cn; fancm@163.com.

Acknowledgments

This work is supported by the National Natural Science Foundation of China (No. 21506144, 21676178, 21706179), the Natural Science Foundation of Shanxi Province (201701D221037), the Foundation of State Key Laboratory of Coal Conversion (J18-19-605).

With the extensive application of photoelectric catalysis in various fields, the electron behaviors are of obvious importance to investigate the mechanism of photoelectrochemistry[1-3]. The quantization of the electron behaviors will display an intuitionistic observation plat to reveal the photocatalytic mechanism. Density-functional theory (DFT), as one of the solutions to the Schrödinger equation as shown in Eqs.(1-2), is usually employed exclusively for the treatment of electronic behaviors, such as the band structure, density of states and even electronic transportation behaviors through interface[4, 5]. And the properties of the electronic ground states and excited states could also be shown in a direct or indirect way by the calculation of DFT[6, 7].

$$\mathrm{E}(\rho)=\mathrm{T}(\rho)+\mathrm{U}(\rho)+\mathrm{E}_{\mathrm{XC}}(\rho) \tag{1}$$

Where, $\mathrm{E}(\rho)$ is the total energy. The terms on the right are, in order, the kinetic energy of a system of non-interacting particles of density ρ, the classical electrostatic energy due to coulombic interactions and all many-body contributions to the total energy, in particular, the exchange and correlation energies.

$$[-\frac{\nabla^2}{2}+V(\boldsymbol{r})+V_H(\boldsymbol{r})+V_{XC}(\boldsymbol{r})]\varphi_i(\boldsymbol{r})=\epsilon_i\varphi_i(\boldsymbol{r}) \tag{2}$$

Here, ϵ_i and $\varphi_i(\boldsymbol{r})$ are occupied KS eigenvalues and eigenstates, respectively. $V(\boldsymbol{r})$ and $V_H(\boldsymbol{r})$ are the ionic and Hartree potentials, respectively, and $V_{XC}(\boldsymbol{r})=\delta\mathrm{E}_{\mathrm{XC}}(\rho)/\delta\rho$ is the exchange–correlation potential. When the molecular orbitals are orthonormal, the $\rho(\boldsymbol{r})$ could be defined as follows.

$$\rho(\boldsymbol{r})=\sum_{\mathrm{i}}|\varphi_{\mathrm{i}}(\boldsymbol{r})|^2 \tag{3}$$

By solving the Schrödinger equations, the electron properties and the total electron density (TED) of any suitable system could be easily displayed. As usual, the situations where DFT calculations have limited accuracy in the calculation of electronic excited states because of the assumption of wave functions of electron density which are named spin-restricted as shown in Eq.(3). Nevertheless, the $\varphi_{\mathrm{i}}(\boldsymbol{r})$ is based on molecular orbital (MO)[8], which is a mathematical function describing the wave-like behavior of an electron in a molecule[9]. This function could be used to investigate the chemical or physical properties through the calculation of the electron properties. The MOs may be occupied by spin-up (α) or spin-down (β) electrons. The same φ_i for both α and β electrons is known as a spin-restricted calculation, and the different φ_i for α and β electrons is named as a spin-unrestricted or spin-polarized calculation. In the unrestricted case, α MOs and β MOs could be defined to form two different charge densities, and their sum show the total charge density and their difference display the spin density. The excited states always mean that the electrons are excited from ground-states, so the partially spin-restricted wave function could be used to define the excitation states[8, 10], as illustrated in Fig.1. When the scattered energy is absorbed by electrons, the electrons will be excited to the higher MO, and the electron states and the multiplicity of the system can be to raise[11]. The ground state always performs the lowest formation energy, which could be calculated through structural optimization analysis. Besides, the multiplicities of ground-state and excited-state can be confirmed. Therefore, a suitable multiplicity state of spin-unrestricted calculation could provide a picture of electrons distribution changes.

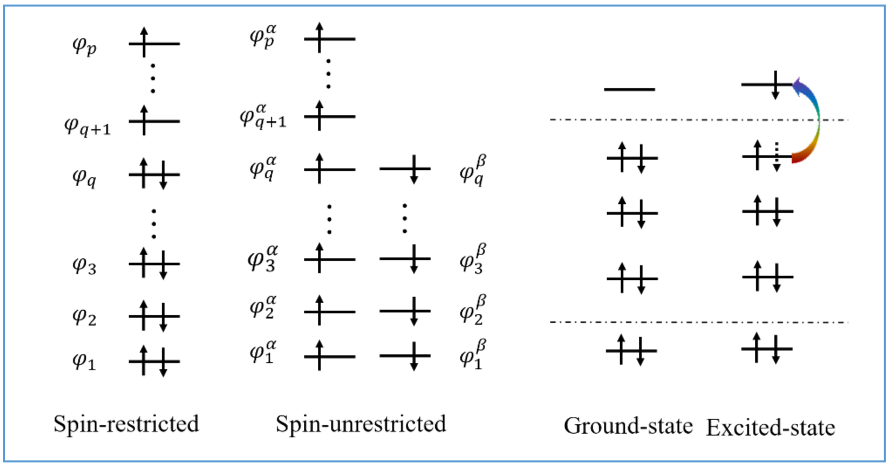

Fig.1. Schematic illustration of the electron for spin-restricted, spin-unrestricted and ground-state, excited-state

The BIOVIA Materials Studio DMoL^3 module is used for offering an effective method to investigate the electronic behaviors, such as the deformation density, Mulliken population analysis and the electron density difference to directly or indirectly provide the electron transfer process (ETP). As with photoelectric catalysis, the ground-state properties have been widely studied. However, very little information is available in the description of processes such as charge carrier generation, transport, and recombination[12], which requires a detailed understanding of several excited-state properties. Although recent studies observed the bulk charge separation of BiOX, for instance, the internal electric field affected electrons should tend to migrate to the surface[13, 14], little was known about electron-transfer processes on their surfaces. To describe the surface-electron-transfer processes, theoretical calculations on the Mulliken population analysis[15, 16], deformation density, the electron density difference were carried out to understand the ETP in detail.

Mulliken charges

Mulliken charges used to be carried out from the Mulliken population analysis[15, 16] by computational chemistry based on the linear combination of atomic orbitals method. Moreover, the Mulliken charges could estimate the partial atomic charges to evaluate electron gain or loss capacity.

Difference distance of A and B atoms (ΔD_{AB})

The difference distance of A and B atoms (ΔD_{AB}) could be calculated by the A—B distance (D_{AB}) minus their Van der Waals radius (r_A, r_B), as shown in Eq.(4).

$$\Delta D_{AB}=D_{AB}-r_A-r_B \quad (4)$$

Deformation density (DD)

The deformation density based on the electron density distribution could be used to produce theoretical dynamic deformation density maps of BiOX. The deformation density is the difference between the molecular and the unrelaxed atomic charge densities, which could tell us the formation of the bonds between atoms[17, 18], as shown Eq.(5).

$$\rho_d(\boldsymbol{r}) = \rho(\boldsymbol{r}) - \sum_\alpha \rho_\alpha(\boldsymbol{r} - \boldsymbol{R}_\alpha) \quad (5)$$

Where $\rho(\boldsymbol{r})$ is the molecular charge density and $\rho_\alpha(\boldsymbol{r} - \boldsymbol{R}_\alpha)$ is the density of the free atom α located at coordinates $\boldsymbol{R}_\alpha$.

Effective mass (m*)

As shown in Eq.(6), m* is estimated by the two order derivative of energy (E) to wave vector (k).

$$m^*=\hbar^2(d^2E/dk^2)^{-1} \quad (6)$$

Electron density difference (EDF)

Caculations about the electron density difference (EDF) through the final state minus the initial state are obtained through Eq.(7) [19].

$$\Delta\rho = \rho_t - \rho_0 \tag{7}$$

Where $\Delta\rho$ is the electron density difference, ρ_t and ρ_0 are the final and initial states of total electron density, respectively.

To gain the initial and final electron density states, the Multiplicity were employed to understand the electron states. Structural optimization analysis of BiOX revealed that the BiOX when the singlet and doublet were employed (Tables S5~S6), which could be regarded as ground/initial states[20]. At the same time, the finitial states were obtained through the introductions of the doublet and triplet.

Supplementary Figures

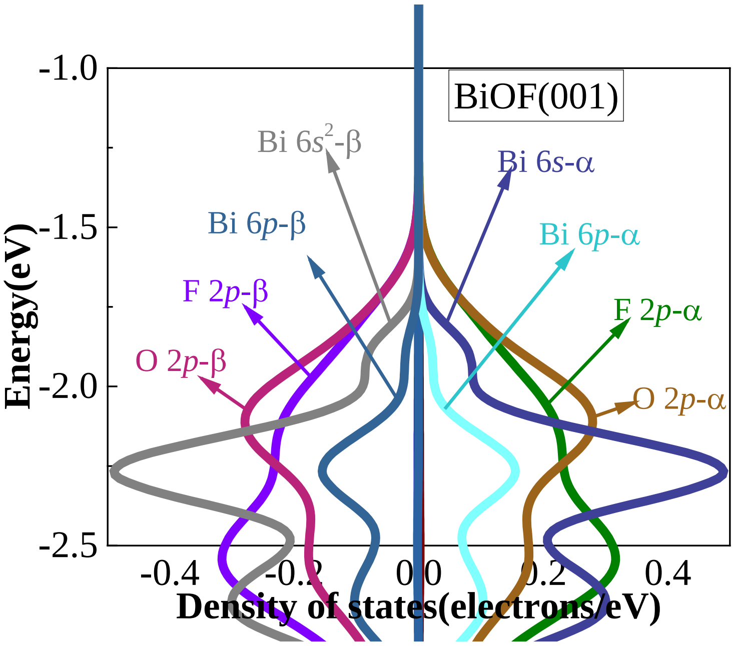

Revised Fig.S1. Density of states around the valance band for BiOF(001) surfaces

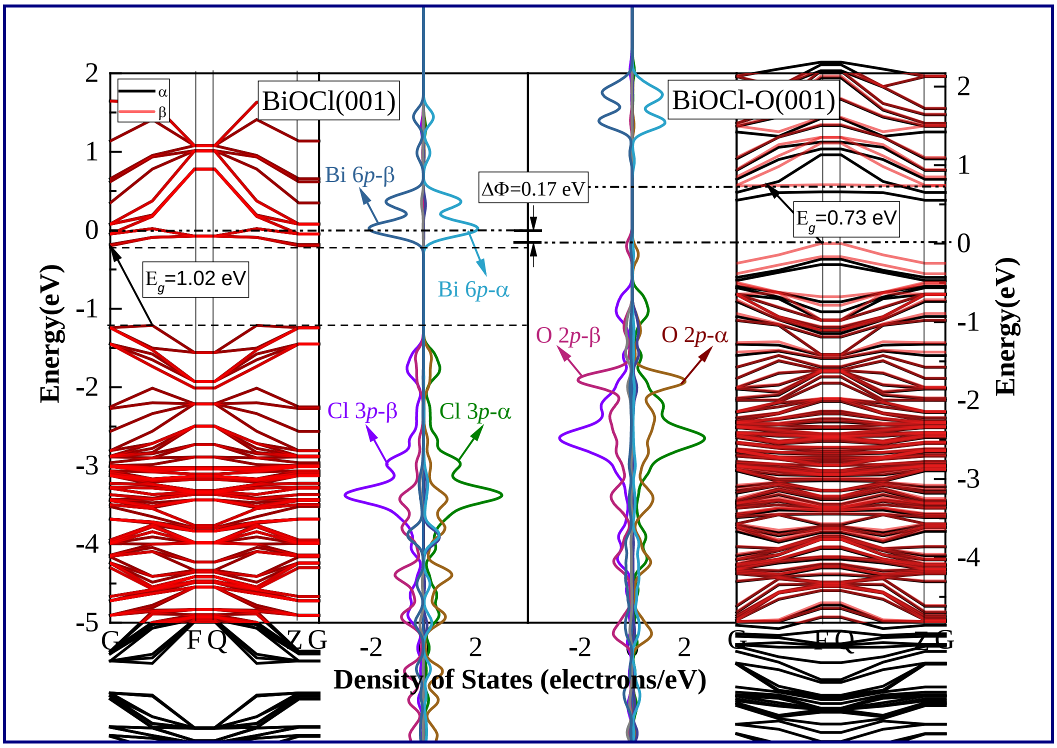

Revised Fig.S2. Band structures and densities of states of BiOCl(001) and BiOCl-O(001) surfaces

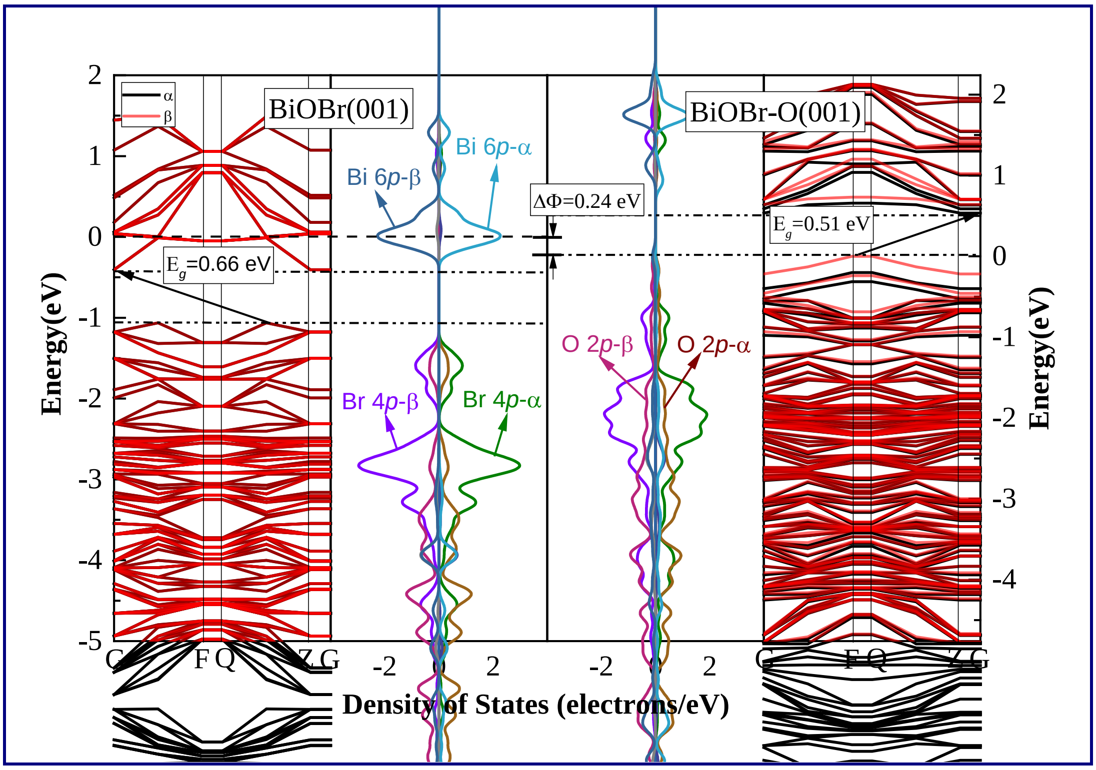

Revised Fig.S3. Band structures and densities of states of BiOBr(001) and BiOBr-O(001) surfaces

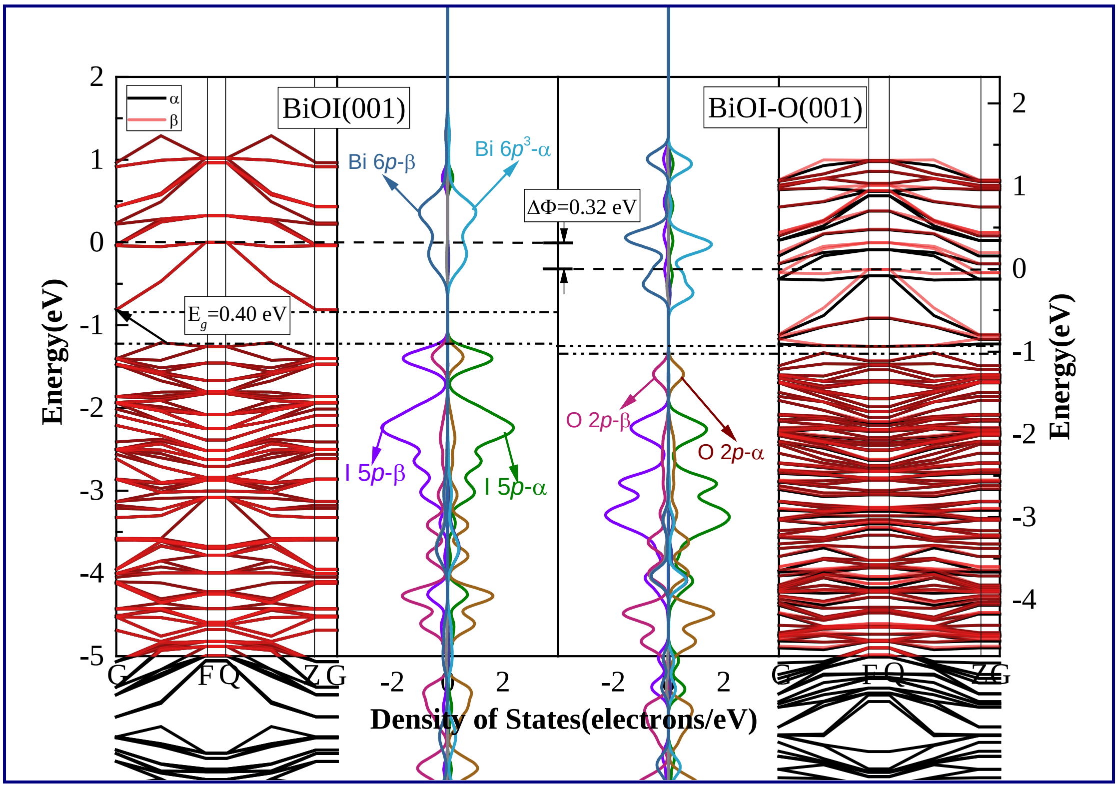

Revised Fig.S4. Band structures and densities of states of BiOI(001) and BiOI-O(001) surfaces

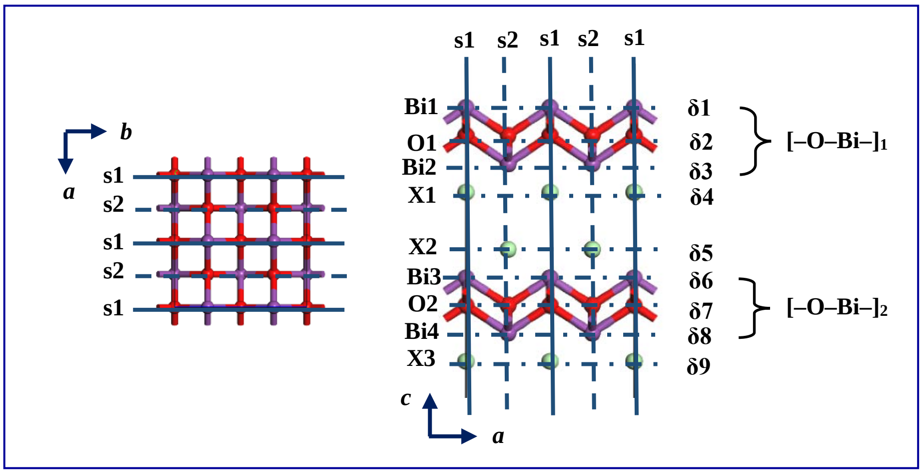

Fig.S5. The layer identifier numbers of BiOX(001) surfaces

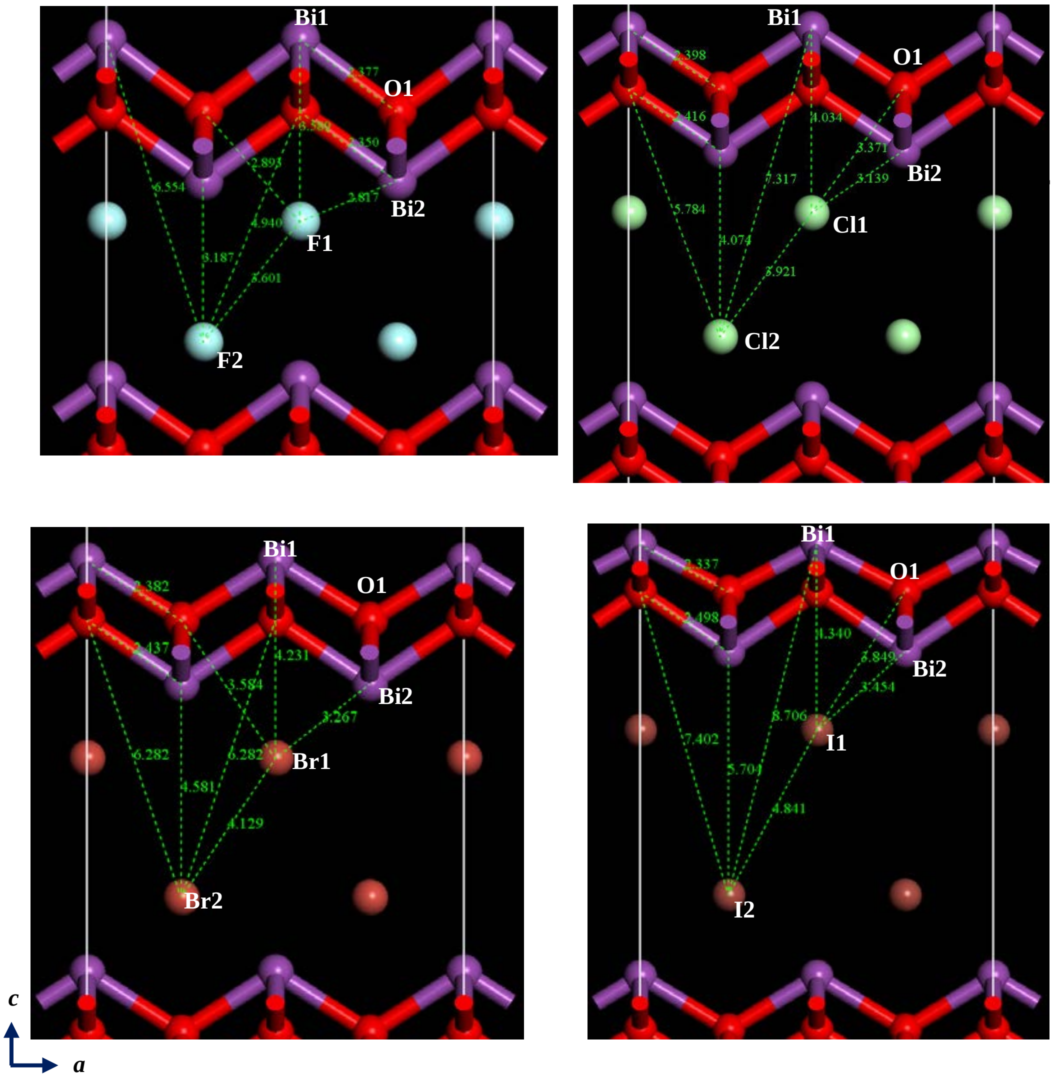

Fig.S6. The distances among F, Cl, Br, I, Bi and O atoms.

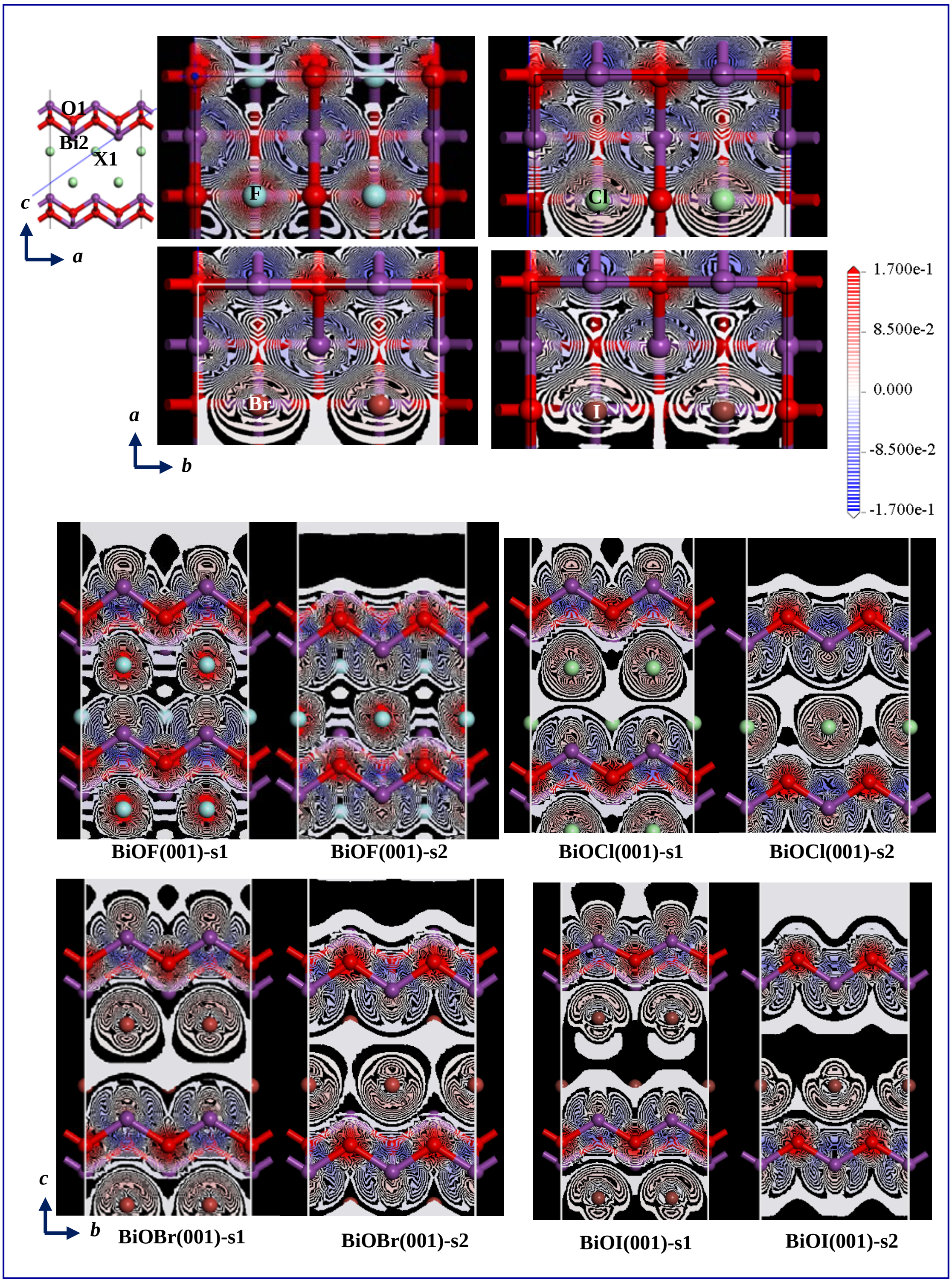

BiOF(001)-s1 BiOF(001)-s2 BiOCl(001)-s1 BiOCl(001)-s2

BiOBr(001)-s1 BiOBr(001)-s2 BiOI(001)-s1 BiOI(001)-s2

Fig.S7. The distributions of equipotential lines of deformation density calculations for BiOX(001) surfaces

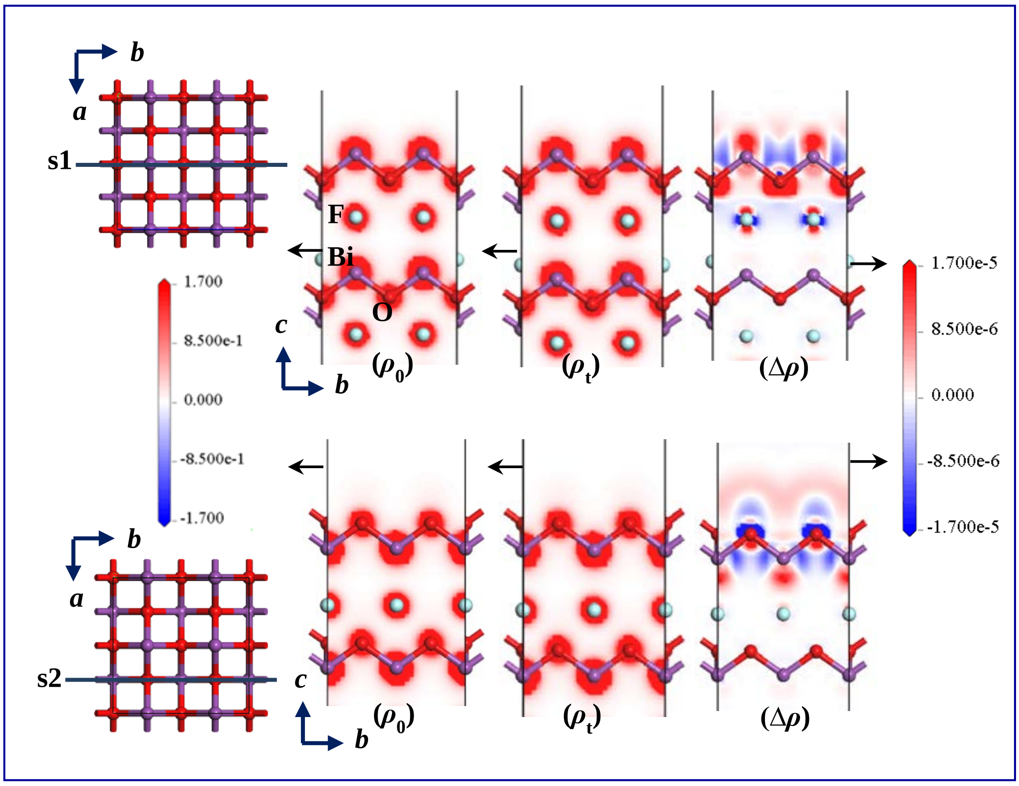

Revised Fig.S8. The total electron densities of initial states (ρ_0) and final states (ρ_t) as well as the electron density difference ($\Delta\rho$, $\Delta\rho=\rho_t-\rho_0$) for BiOF(001) surfaces

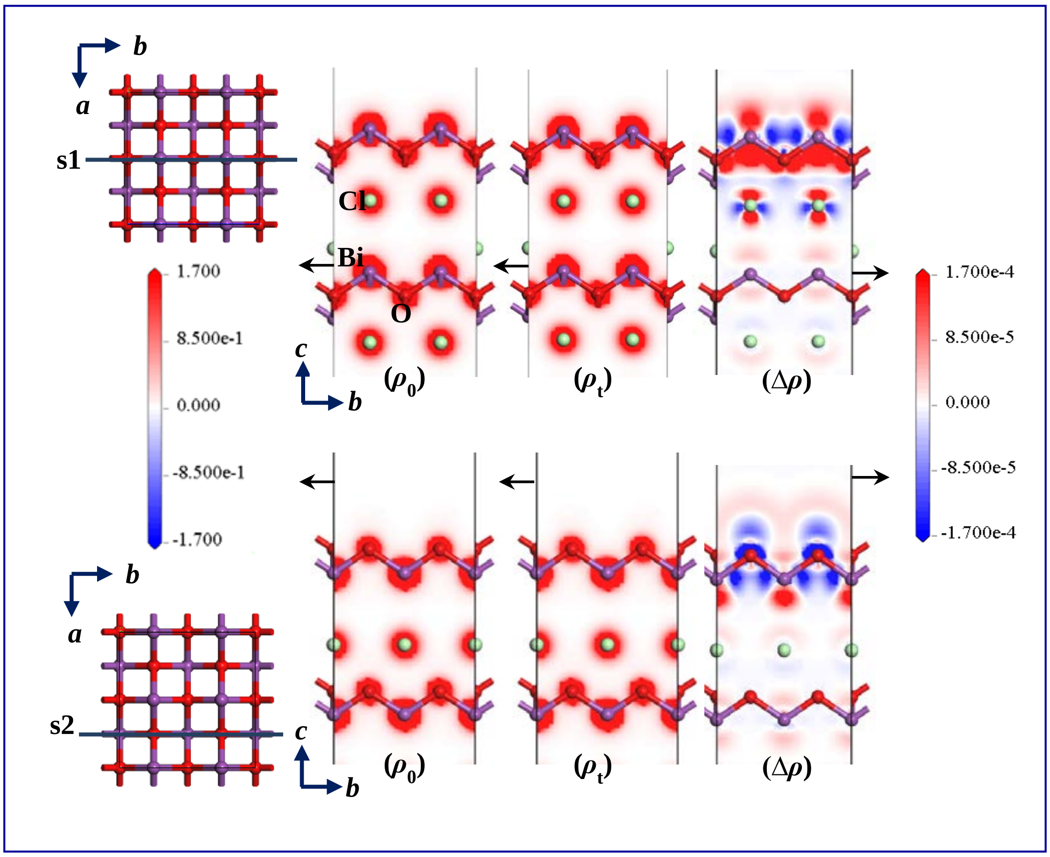

Revised Fig.S9. The total electron densities of initial states (ρ_0) and final states (ρ_t) as well as the electron density difference ($\Delta\rho$, $\Delta\rho=\rho_t-\rho_0$) for BiOCl(001) surfaces

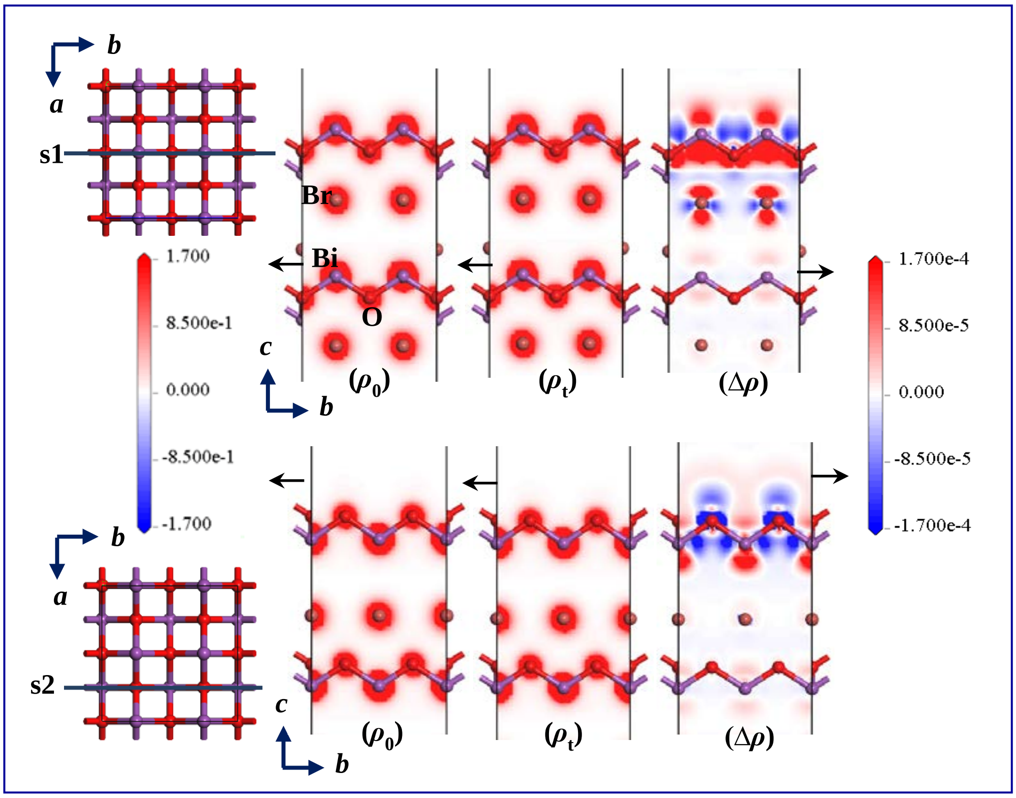

Revised Fig.S10. **The total electron densities of initial states (ρ_0) and final states (ρ_t) as well as the electron density difference ($\Delta\rho$, $\Delta\rho=\rho_t-\rho_0$) for BiOBr(001) surfaces**

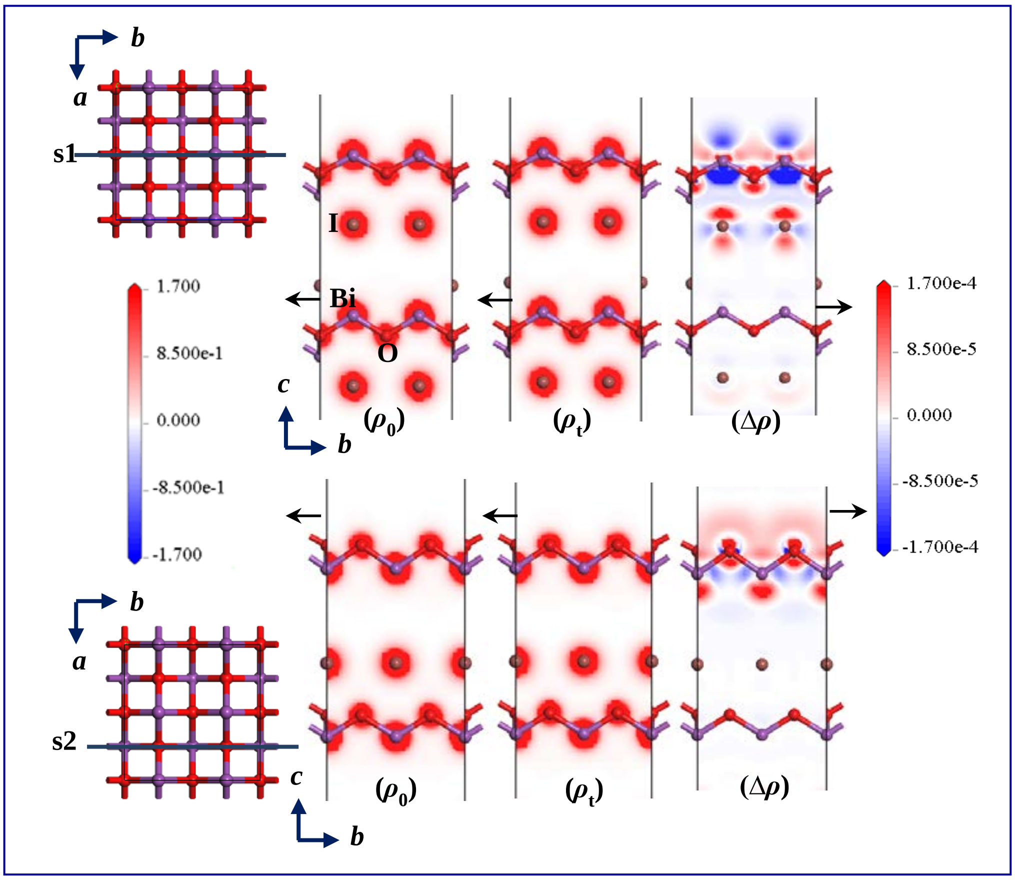

Revised Fig.S11. The total electron densities of initial states (ρ_0) and final states (ρ_t) as well as the electron density difference ($\Delta\rho$, $\Delta\rho=\rho_t-\rho_0$) for BiOI(001) surfaces

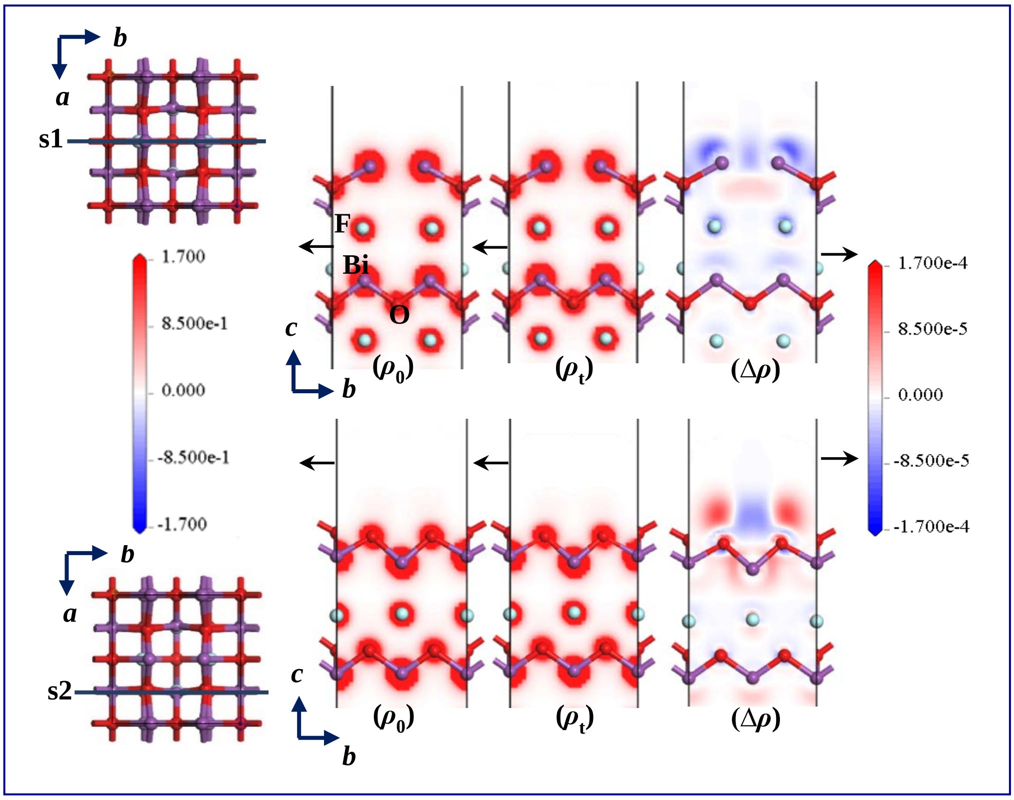

Revised Fig.S12. The total electron densities of initial states (ρ_0) and final states (ρ_t) as well as the electron density difference ($\Delta\rho$, $\Delta\rho=\rho_t-\rho_0$) for BiOF-O(001) surfaces

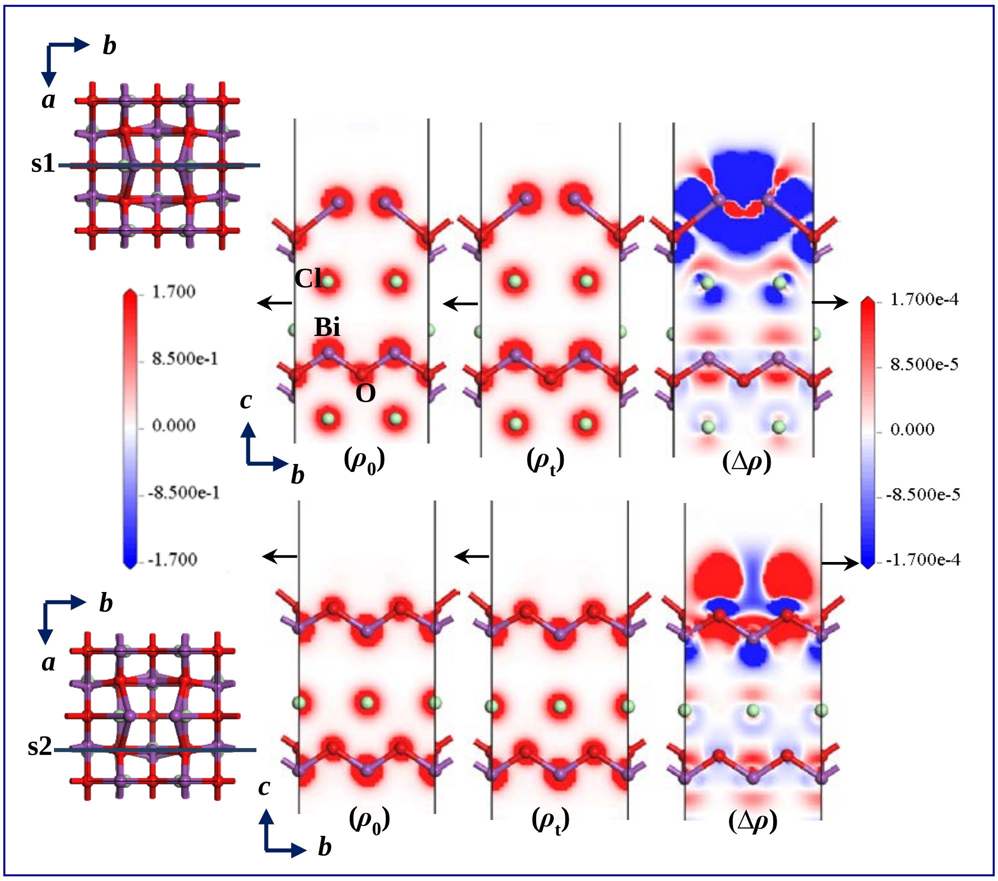

Revised Fig.S13. The total electron densities of initial states (ρ_0) and final states (ρ_t) as well as the electron density difference ($\Delta\rho$, $\Delta\rho=\rho_t-\rho_0$) for BiOCl-O(001) surfaces

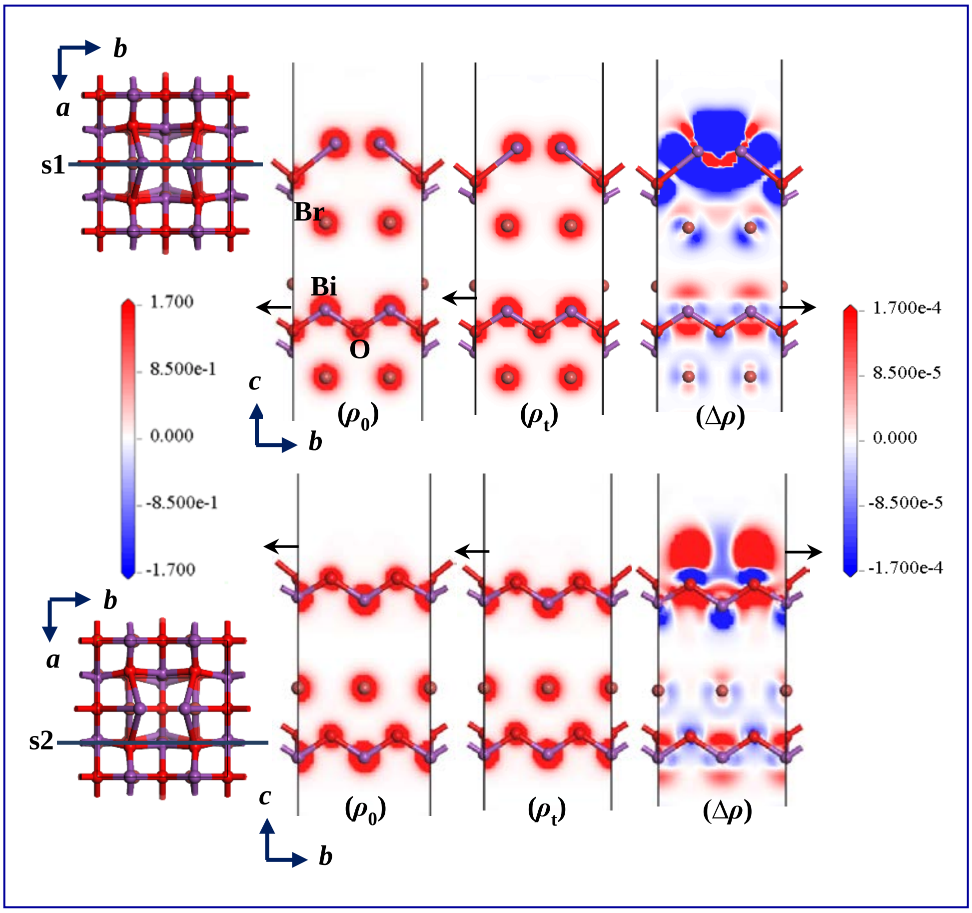

Revised Fig.S14. **The total electron densities of initial states (ρ_0) and final states (ρ_t) as well as the electron density difference ($\Delta\rho$, $\Delta\rho=\rho_t-\rho_0$) for BiOBr-O(001) surfaces**

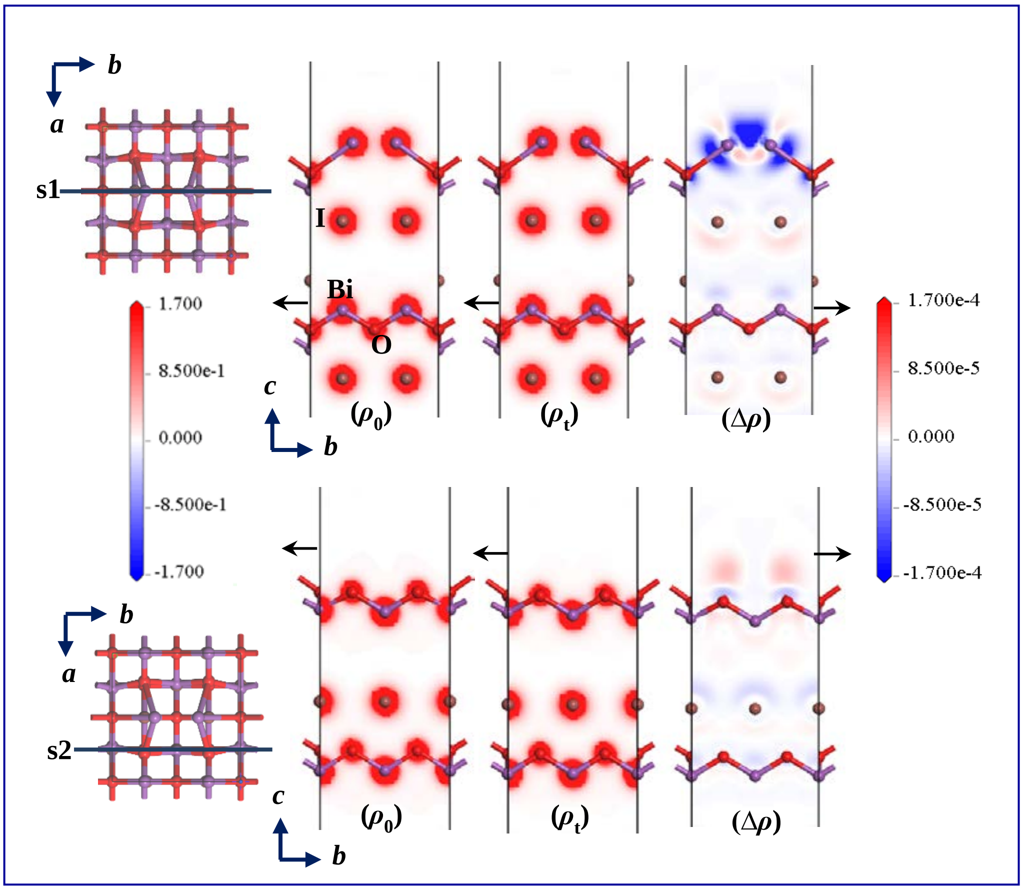

Revised Fig.S15. The total electron densities of initial states (ρ_0) and final states (ρ_t) as well as the electron density difference ($\Delta\rho$, $\Delta\rho=\rho_t-\rho_0$) for BiOI-O(001) surfaces

Table S1. The work functions (Φ) of BiOX(001) and BiOX-O(001) surfaces and the quantity changes (ΔΦ, $\Delta\Phi = \Phi_{\mathrm{BiOX(001)}} - \Phi_{\mathrm{BiOX\text{-}O(001)}}$) between BiOX(001) and BiOX-O(001) surfaces

	Φ(eV)		Φ(eV)		Φ(eV)		Φ(eV)
BiOF(001)	3.40	BiOCl(001)	3.18	BiOBr(001)	3.10	BiOI(001)	2.97
BiOF-O(001)	3.46	BiOCl-O(001)	3.35	BiOBr-O(001)	3.35	BiOI-O(001)	3.29
ΔΦ	0.06	ΔΦ	0.17	ΔΦ	0.24	ΔΦ	0.32

Table S2. The covalent/atom radius, van der Waals radius, Ionic radius and electronegativities of F, Cl, Br, I, O and Bi atoms

	F	Cl	Br	I	O	Bi
Covalent/Atom radius (Å)	0.64[21]	0.99[21]	1.14[21]	1.23[21]	0.66[21]	1.55[21]
Van der Waals radius(Å)	1.47[22]	1.75[22]	1.85[22]	1.98[22]	1.52[22]	2.07[22]
Electronegativity	4.0[23]	3.0[23]	2.8[23]	2.5[23]	3.5[23]	1.9[23]

Table S3. Calculated effective mass ($m^{*} = \hbar^{2}/\frac{d^{2}E}{dk^{2}}$) for electrons ($m_e$*=m*/$m_0$, m_0: the mass of an electron) and holes (m_h*=m*/m_0) along *c* direction

	BiOF	BiOF-O	BiOCl	BiOCl-O	BiOBr	BiOBr-O	BiOI	BiOI-O
m_e*	1.1705	0.0905	0.1857	0.1089	0.0487	0.0889	0.1572	0.0627
m_h*	-0.1524	-0.1974	-0.1175	-0.0651	-0.1125	-2.4802	-0.1664	-0.8035

Table S4. The lattice parameters and surface area values for BiOX(001) surfaces

	BiOF (001)	BiOCl(001)	BiOBr(001)	BiOI(001)
a=b (Å)	7.6372	8.0038	8.0656	8.263
c (Å)	30.8504	33.2861	35.169	34.9483
α=β=γ(°)	90	90	90	90
Surface area value (Å^2/site)	3.65	4.00	4.07	4.27

Table S5. The formation energies (Ha) of BiOX(001) surfaces

	BiOF(001)	BiOCl(001)	BiOBr(001)	BiOI(001)
Singlet	-485787.277021	-491551.276630	-525371.977066	-594911.679096
Doublet	-485787.276721	-491551.276367	-525371.974181	-594911.678719
Triplet	-485787.275766	-491551.275558	-525371.973319	-594911.677569

Table S6. The formation energies (Ha) of BiOX-O(001) surfaces

	BiOF-O(001)	BiOCl-O(001)	BiOBr-O(001)	BiOI-O(001)
Singlet	-485712.095786	-491476.147287	-525296.850320	-594836.557203
Doublet	-485712.096314	-491476.147791	-525296.850857	-594836.557795
Triplet	-485712.094064	-491476.113010	-525296.849245	-594836.555299

References

1. Z. Lin, L. Li, L. Yu, W. Li and G. Yang, *J. Mater. Chem. A*, 2017, **5**, 5235-5259.
2. J. Li, H. Li, G. Zhan and L. Zhang, *Acc Chem Res*, 2017, **50**, 112-121.
3. S. Dadashi-Silab, S. Doran and Y. Yagci, *Chem Rev*, 2016, **116**, 10212-10275.
4. Y. Ping, W. A. Goddard III and G. A. Galli, *J Am Chem Soc*, 2015, **137**, 5264-5267.
5. S. E. Weitzner and I. Dabo, *npj Computational Materials*, 2017, **3**.
6. A. Görling, *Phys Rev A*, 1996, **54**, 3912.
7. P. Verma and D. G. Truhlar, *J Phys Chem Lett*, 2017, **8**, 380-387.
8. J. A. Pople and R. K. Nesbet, *J Chem Phys*, 1954, **22**, 571-572.
9. R. S. Mulliken, *Physical Review*, 1932, **41**, 49-71.
10. Glushkov, *Computing Letters*, 2007, **3**, 65-69.
11. P. B. Armentrout, *Science*, 1991, **251**, 175-179.
12. L. Kronik and J. B. Neaton, *Annu Rev Phys Chem*, 2016, **67**, 587-616.
13. J. Li, L. Cai, J. Shang, Y. Yu and L. Zhang, *Adv Mater*, 2016, **28**, 4059-4064.
14. X. a. Dong, W. Zhang, Y. Sun, J. Li, W. Cen, Z. Cui, H. Huang and F. Dong, *J Catal*, 2018, **357**, 41-50.
15. R. S. Mulliken, *J Chem Phys*, 1955, **23**, 1833-1840.
16. R. S. Mulliken, *J Chem Phys*, 1955, **23**, 1841-1846.
17. B. Delley, *Chem Phys*, 1986, **110**, 329-338.
18. W. Schwarz, K. Ruedenberg and L. Mensching, *J Am Chem Soc*, 1989, **111**, 6926-6933.
19. D. Cremer and E. Kraka, *Angew. Chem. Int. Ed.*, 1984, **23**, 627-628.
20. X. Zhang, G. Li, C. Fan, G. Ding, Y. Wang and P. Han, *Comp Mater Sci*, 2014, **95**, 113-120.
21. J. A. Dean, *Lange's handbook of chemistry, Fifteenth Edition*, McGraw-Hill, Inc., 1999.
22. W. M. Haynes, *CRC handbook of chemistry and physics*, CRC press, Boca Raton, 2016.
23. J. E. McMurry, R. C. Fay, J. K. Robinson and J. Topich, *Chemistry, Seven edition*, Pearson, June 22, 2015.